



Regular Paper

pISSN: 1229-7607

eISSN: 2092-7592

DOI: <https://doi.org/10.4313/TEEM.2017.18.6.316>OAK Central: <http://central.oak.go.kr>

Influence of Trap Passivation by Hydrogen on the Electrical Properties of Polysilicon-Based MSM Photodetector

Jae-Sung Lee[†]*Division of Green Energy Engineering, Uiduk University, Gyeongju 38004, Korea*

Received September 19, 2016; Revised July 16, 2017; Accepted July 21, 2017

A new approach to improving the electrical characteristics and optical response of a polysilicon-based metal-semiconductor-metal (MSM) photodetector is proposed. To understand the cause of current restriction in the MSM photodetector, modified trap mechanisms are suggested, which include interfacial electron traps at the metal/polysilicon interface and silicon dangling bonds between silicon crystallite grains. Those traps were passivated using hydrogen ion implantation with subsequent post-annealing. Photodetectors that were ion-implanted under optimal conditions exhibited improved photoconductivity and reduced dark current instability, implying that the hydrogen bonds in the polysilicon influence the simultaneous decreases in the density of dangling bonds at grain boundaries and the trapped positive charges at the contact interface.

Keywords: Metal-semiconductor-metal (MSM) photodetector, Hydrogen ion implantation, Trap passivation, Photoconductivity

1. INTRODUCTION

Silicon photodetectors are important devices that are widely used in microelectronics, telecommunications, and biological and chemical sensing [1-3]. One of the most common silicon photodetectors is a metal-semiconductor-metal (MSM) structure composed of two Schottky barriers with polysilicon between them. The Schottky barrier exhibits a bias-induced, time-dependent reverse current, indicating that the sensitivity of the sensor may be limited because of variations in the reverse current over time. The main components of the reverse current are thermionic emission and tunneling, and they vary because of charge trapping at the interface. The thin polysilicon layer often used as an absorption layer in MSM photodetectors, is composed of silicon crystallites with grain boundaries. Defects caused by incomplete atomic bonding and disordered material at the grain boundaries result in trapping

states that reduce the number of carriers and a potential barrier that impedes carrier motion. To minimize the effect of charge trapping and/or charged defects, either they or their electrical activity must be eliminated.

In an earlier study, electrical conduction in polysilicon was established using grain boundary scattering models [4], and hydrogen passivation of polysilicon grain boundaries was studied in research on thin-film transistors and photovoltaics [5,6]. Some papers discussed the reverse current mechanisms in silicon-based MSM photodetectors for applications in digital imaging and optical communications [7,8]. We also studied deuterium passivation of grain boundary traps in a polysilicon-based MSM photodetector [9]. However, these previous studies provided different approaches to understanding the behavior of the traps existing at the contact interfaces and grain boundaries. When the same trap-generation mechanism is applied to these two areas, the trap density can be decreased concurrently by one method. We suggested the hydrogen implantation process for this purpose. This approach has not yet been announced by other groups.

In most practical metal/semiconductor interfaces, the semiconductor surface contains a thin insulating oxide layer, which is often referred to as an interfacial layer with surface states [10]. Passivation of interfacial surface states through amphoteric defect reactions can

[†] Author to whom all correspondence should be addressed:

E-mail: jaesung@uu.ac.kr

Copyright ©2017 KIEEME. All rights reserved.

This is an open-access article distributed under the terms of the Creative Commons Attribution Non-Commercial License (<http://creativecommons.org/licenses/by-nc/3.0>) which permits unrestricted noncommercial use, distribution, and reproduction in any medium, provided the original work is properly cited.

change the barrier width at a metal/polysilicon interface. Potential barriers arise at the grain boundaries because of unsatisfied silicon bonds between the grains. This is also conceptually similar to the generation of surface states at the silicon/oxide interface in metal oxide semiconductor (MOS) devices. When the unsatisfied silicon bonds are passivated with appropriate atoms, the potential barrier at the grain boundaries can be lowered to meet the current level.

This research reports work that is part of a project to develop an evanescent coupling sensor consisting of a waveguide core and an MSM photodetector. To improve the photoconductivity and reduce the dark current instability in the MSM photodetector, we introduced a hydrogen bond for passivation of the surface states and/or the traps existing at both interface and grain boundary barriers. Hydrogen was incorporated into the polysilicon through ion implantation with subsequent post-annealing. Considering the passivation effect of hydrogen, we also mention physical models for the traps located at the contact interface and grain boundaries.

2. EXPERIMENTS

In a biosensor application, detectors are not necessarily used in an interdigitated electrode pattern. This study used a coplanar photodetector structure in which two electrodes were placed directly on the polysilicon absorption layer. MSM photodetectors were fabricated by a standard silicon process. A 400 nm thick thermal-oxide layer was grown on top of the silicon substrate, followed by a 500 nm thick layer of undoped polysilicon deposited by low-pressure chemical vapor deposition. The metal electrodes were comprised of 200 nm of Ti on the bottom and 500 nm of Al on top. Ti was chosen as the barrier metal because it produces an interface barrier with a height approximately equal to one-half the bandgap of silicon, and it offers excellent adhesion to silicon. The structure has an active area of 2,500 μm^2 . An antireflection (AR) coating of 150 nm thick SiO_2 was deposited on the structure's active area. Figure 1 shows a top view of the metal pads in the MSM photodetector. The dotted box in the enlarged figure represents the active area for light absorption.

After metallization, hydrogen was incorporated into the MSM structure through hydrogen ion implantation. Hydrogen ions (H^+) were implanted at energies of 11–27 keV, and the ion dose was fixed at $10^{14}/\text{cm}^2$. The optima condition for ion implantation on this device structure was calculated using a commercial tool (SRIM) so that the peak of the H^+ distribution was located inside the polysilicon layer. Hydrogen ions in the polysilicon were activated through N_2 -ambient post-annealing at 400 $^\circ\text{C}$. For comparison, a control device annealed only in N_2 -ambient, a hydrogen-annealed device annealed only in H_2 ambient, and an Ar-implanted device were prepared. Ion implantation was usually followed by subsequent post-annealing. The energy of Ar implantation was adjusted to obtain the same ion range as in hydrogen implantation to show the different effect of the two atoms on the electrical conduction. A light-emitting diode with a

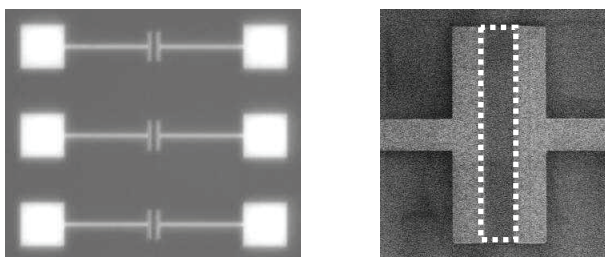


Fig. 1. Top view of the metal pads in the fabricated MSM photodetector. Dotted box represents the active area for light absorption.

wavelength of 850 nm was used for illumination.

3. RESULTS AND DISCUSSION

Figure 2 compares the photocurrent and dark current for the hydrogen-implanted, hydrogen-annealed, and control devices. After hydrogen implantation, the device shows a relatively low dark current and high photocurrent, implying that some portion of the interface traps at polysilicon grain boundaries and/or the metal/polysilicon interfaces was passivated. In the dark current evaluation, the interface barrier height of the hydrogen-implanted device was as much as 0.05 eV higher than that of the control device. However, atomic depth profile analysis of the hydrogen-annealed device showed that hydrogen accumulated near the AR/polysilicon interface. This was caused by the difference in diffusion coefficients between SiO_2 ($10^{-11} \text{ cm}^2/\text{s}$) and Si ($10^{-15} \text{ cm}^2/\text{s}$) [11]. Therefore, slight passivation of the traps was achieved by hydrogen annealing.

Under illumination, the concentration of electron-hole pairs consists of the equilibrium (dark) and photo excited carrier concentrations. Correspondingly, the measured photocurrent (I_{ph}) is the sum of the dark current and photo excited current (I_{ex}). Figure 3 shows the responsivity, which is the ratio of the photo excited

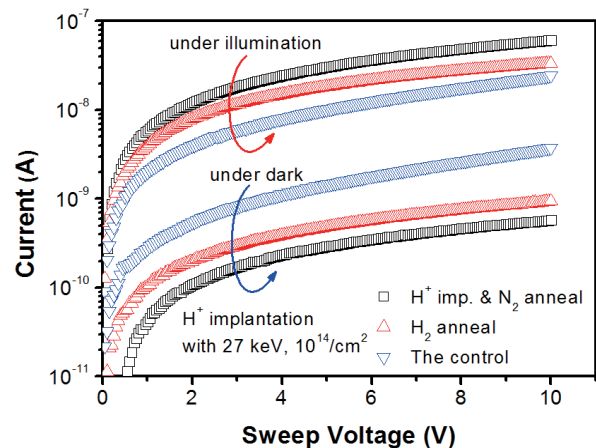


Fig. 2. Comparison of photocurrent and dark current for the hydrogen-implanted, hydrogen-annealed, and control devices.

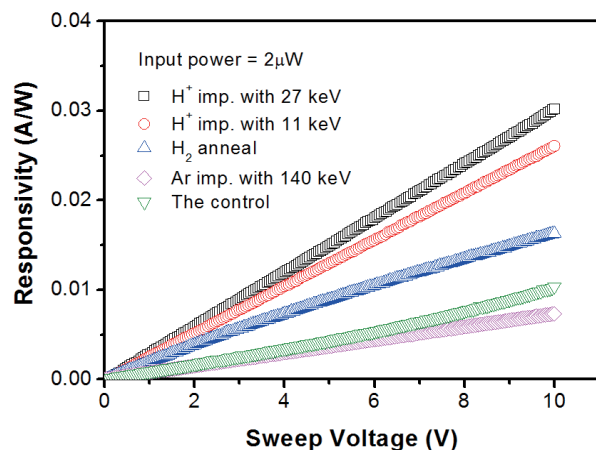


Fig. 3. Responsivity as a function of bias voltage for the hydrogen-implanted, hydrogen-annealed, Ar-implanted, and control devices. The gap between electrodes was 50 μm .

current to the incident optical power, for all of the devices. The responsivity shows a quasi-linear dependence on the bias voltage. This indicates that the Ti/polysilicon interface in this study formed a semi-Schottky contact. In addition, the responsivity of all the devices was rather low compared to that of devices in previous studies [2,7] because the measured device had a long gap ($L = 50 \mu\text{m}$) between the two electrodes; however, a passivation effect was observed in the large absorption layer. Among the fabricated devices, the device with hydrogenated polysilicon developed by ion implantation shows increased responsivity, which is approximately three times that of the control device. This indicates that the photoconductive gain, which is proportional to the ratio of the carrier recombination lifetimes to the transit time between the two electrodes, was increased by hydrogen ion implantation and subsequent post-annealing. Passivation of some traps at the grain boundaries has the advantage of increasing the traveling path of photo generated carriers in polysilicon. In the Ar-implanted device, the total electrical resistance of the polysilicon layer increased. The heavy Ar ions would disorder some of the silicon bonds in the crystallite grains during ion implantation.

Figure 4 shows that the I_{ex} -to-dark-current ratio, which is used to consider the noise and signal detection threshold for sensor applications, was improved by hydrogen implantation and subsequent annealing. When the total film thickness on the silicon wafer is considered, the peaks of the ion distribution at 11 and 27

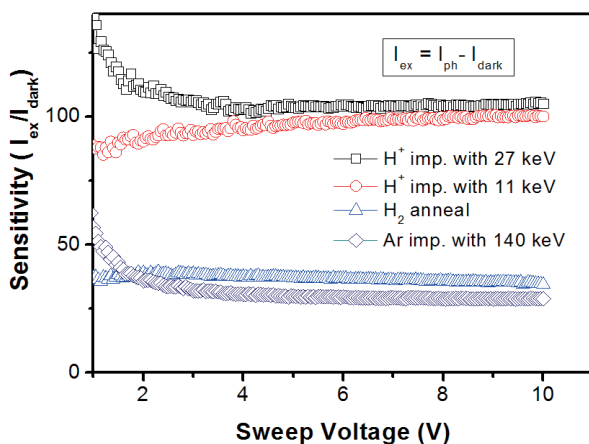


Fig. 4. Photo excited-current-to-dark-current ratio for the hydrogen-implanted, hydrogen-annealed, and Ar-implanted devices. Photo excited current is the current excluding the dark current.

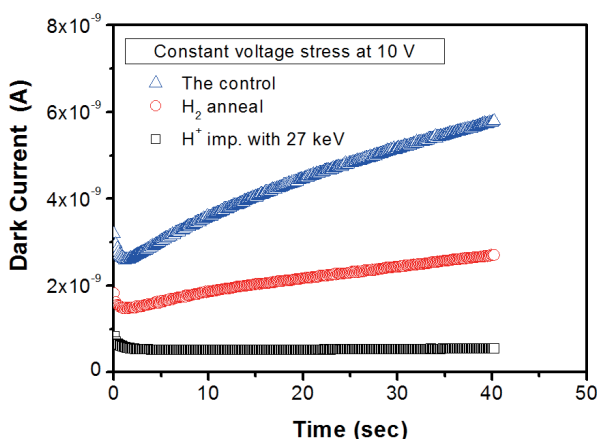


Fig. 5. Instability of dark current under constant bias voltage of 10 V for the hydrogen-implanted, hydrogen-annealed, and control devices.

keV are found to be located near the top and in the middle of the polysilicon layer, respectively. The hydrogen ions would be diffused toward the polysilicon bulk and activated by forming chemical bonds with defects through post-annealing.

The dark current at the metal/semiconductor interface barrier grows unstable over time. The prevailing sources of dark current are tunneling and thermionic emission. The instability is due to the release of trapped charges over time at the metal/semiconductor interface, which reduces the barrier width and increases the tunneling rate through the barrier. The increase in the tunneling current can be explained by a phenomenon similar to trap-assisted tunneling in a MOS system [12]. The generation of a neutron electron trap and/or hole trapping at the cathode junction allows more dark current to flow through the interface barrier. Interface traps inactivated by hydrogen passivation will not contribute to the increase in dark current for a constant voltage bias. Figure 5 shows the dark current instabilities of the MSM photodetectors biased at 10 V. In the hydrogen-implanted device, as a hydrogen bond was generated at the interface and eliminated the electrical activity of the interface trap, generation of hole trapping was suppressed during the bias time. However, for the hydrogen-annealed device, only a small number of hydrogen atoms reached the metal/semiconductor interface because of the presence of the blocking-metal layer on the polysilicon film.

In a polysilicon-based MSM photodetector, current flow is restricted by both interface and bulk-limited conduction because conduction occurs across two metal/polysilicon interface barriers and many grains or grain boundaries. Ideally, the interface barrier height is related to the difference between the metal's work function and semiconductor affinity, and is therefore a constant. Undoped polysilicon conduction in an MSM photodetector depends on the transport within the grain boundaries and the crystallites between grain boundaries. When the trapping sites at the grain boundary are saturated or diminished, the crystallite resistivity in the grains will be the main contributor to the voltage drop across the polysilicon.

Physical models of the polysilicon grain boundary and metal/polysilicon contact based on the experimental results can be described as follows. The trapping sites in the grain boundaries are usually ascribed to silicon dangling bonds, which also play an important role at the Si/SiO₂ interface [13]. When we assume a thin SiO₂ layer between the grains and then make the thickness of the SiO₂ approach zero, the interface traps between the grains will directly influence the carrier transport through the entire polysilicon layer. Regarding the metal/polysilicon interface, it is well known that the barrier heights of freshly prepared metal/Si contacts are very sensitive to the condition of the Si surface before metal preparation [14]. When this is also true for an Al/Ti-polysilicon contact, the generation of a thin oxide layer at the Ti/polysilicon interface owing to the high reactivity of Ti with O₂ will be noticeable. The oxide layer contains trapped charges that affect the barrier height. Neutral electron traps that act as stepping stones for tunneling carriers could be generated by hole trapping in trivalent silicons or broken Si-O sites at the metal/polysilicon interface [15]. The width of the interface barrier at the cathode is determined by the density of the trapped positive charges. Therefore, according to the modified trap concept, the quantity of dangling bonds and degree of hole trapping could possibly be decreased concurrently by hydrogen passivation.

4. CONCLUSIONS

Electrical conduction at a metal/polysilicon interface barrier can be explained by trap-assisted tunneling, which is thought to be the mechanism of thin dielectric film degradation, whereas the structural disorder at polysilicon grain boundaries is likely to be similar to the atomic disorder at the Si/SiO₂ interface in a MOS structure. Under

these trap models, hydrogen passivation was introduced by ion implantation and subsequent post-annealing. Measurements of hydrogen-implanted devices demonstrated improved responsivity and sensitivity and reduced dark current instability compared to those of devices obtained by other processes. Therefore, it is thought that a substantially greater portion of the interfacial electron traps and dangling bonds present in the polysilicon-based MSM structure were passivated, thus enhancing the performance of the photodetector.

ACKNOWLEDGMENTS

This research was supported by the Basic Science Research Program through the National Research Foundation of Korea (NRF) funded by the Ministry of Education (No. 2017R1D1A3B03032478) and by the Nano-Material Technology Development Program through the NRF funded by the Ministry of Science, ICT and Future Planning (2009-0082580). The author thanks KOMAC for assistance with ion implantation.

REFERENCES

- [1] M. Casalino, L. Sireto, L. Moretti, and I. Rendina, *Semicond. Sci. Technol.*, **23**, 075001 (2008). [DOI: <https://doi.org/10.1088/0268-1242/23/7/075001>]
- [2] R. Pownall, G. Yuan, T. W. Chen, P. Nikkel, and K. L. Lear, *IEEE Photonics Technol. Lett.*, **19**, 513 (2007). [DOI: <https://doi.org/10.1109/LPT.2007.893573>]
- [3] L. Pancheri, M. Scandiuazzo, G.F.D. Betta, D. Stoppa, F. De Nisi, L. Gonzo, and A. Simoni, *Solid-State Electro.*, **49**, 175 (2005). [DOI: <https://doi.org/10.1016/j.sse.2004.08.010>]
- [4] H. Marom, M. Ritterband, and M. Eizenberg, *Thin Solid Films*, **510**, 62 (2006). [DOI: <https://doi.org/10.1016/j.tsf.2005.12.155>]
- [5] J. Chen, D. Yang, Z. Xi, and T. Sekiguchi, *Physica B: Condensed Matter*, **364**, 162 (2005). [DOI: <https://doi.org/10.1016/j.physb.2005.04.008>]
- [6] W. Wang, L. Wang, F. Liu, F. Yan, S. Johnston, and M. Al-Jassim, *Proc. 2012 38th IEEE Photovoltaic Specialists Conference* (IEEE, Austin, USA, 2012) p. 001144. [DOI: <https://doi.org/10.1109/PVSC.2012.6317804>]
- [7] S. Ghanbarzadeh, S. Abbaszadeh, and K. S. Karim, *IEEE Electron Device Lett.*, **35**, 235 (2014). [DOI: <https://doi.org/10.1109/LED.2013.2295976>]
- [8] R. P. MacDonald, N. G. Tarr, B. A. Syrett, S. A. Boothroyd, and J. Chrostowski, *IEEE Photonics Technol. Lett.*, **11**, 108 (1999). [DOI: <https://doi.org/10.1109/68.736410>]
- [9] J. S. Lee, *J. Nanosci. Nanotechnol.*, **16**, 6193 (2016). [DOI: <https://doi.org/10.1166/jnn.2016.12109>]
- [10] E. H. Rhoderick and R. H. Williams, *Metal-semiconductor Contacts*, 2nd ed. (Clarendon Press, Oxford, 1988) p. 11.
- [11] R. W. Lee, R. C. Frank, and D. E. Swets, *J. Chem. Phys.*, **36**, 1062 (1962). [DOI: <https://doi.org/10.1063/1.1732632>]
- [12] L. Larcher, *IEEE Trans. Electron Devices*, **50**, 1246 (2003). [DOI: <https://doi.org/10.1109/TED.2003.813236>]
- [13] J. S. Lee, *Trans. Electr. Electron. Mater.*, **13**, 188 (2012). [DOI: <https://doi.org/10.4313/TEEM.2012.13.4.188>]
- [14] H. C. Card, *IEEE Trans. Electron Devices*, **23**, 538 (1976). [DOI: <https://doi.org/10.1109/T-ED.1976.18449>]
- [15] H. Uchida and T. Ajioka, *Appl. Phys. Lett.*, **51**, 433 (1987). [DOI: <https://doi.org/10.1063/1.98413>]